MOLECULAR AND CELLULAR BIOLOGY, July 2006, p. 5249–5258 Vol. 26, No. 14
0270-7306/06/$08.00+0 doi:10.1128/MCB.02473-05

The Scaffold Protein Cybr Is Required for Cytokine-Modulated Trafficking of Leukocytes In Vivo

Vincenzo Coppola,[1]* Colleen A. Barrick,[1] Sara Bobisse,[2,3] Maria Cecilia Rodriguez-Galan,[4] Michela Pivetta,[2,3] Della Reynolds,[4] O. M. Zack Howard,[5] Mary Ellen Palko,[1] Pedro F. Esteban,[1] Howard A. Young,[4] Antonio Rosato,[2,3] and Lino Tessarollo[1]*

Neural Development Group, Mouse Cancer Genetics Program,[1] Laboratory of Experimental Immunology,[4] and Laboratory of Molecular Immunoregulation,[5] Center for Cancer Research, National Cancer Institute, Frederick, Maryland, and Department of Oncology and Surgical Sciences, University of Padova,[2] and Istituto Oncologico Veneto,[3] Padova, Italy

Received 27 December 2005/Returned for modification 31 January 2006/Accepted 27 April 2006

Trafficking and cell adhesion are key properties of cells of the immune system. However, the molecular pathways that control these cellular behaviors are still poorly understood. Cybr is a scaffold protein highly expressed in the hematopoietic/immune system whose physiological role is still unknown. In vitro studies have shown it regulates LFA-1, a crucial molecule in lymphocyte attachment and migration. Cybr also binds cytohesin-1, a guanine nucleotide exchange factor for the ARF GTPases, which affects actin cytoskeleton remodeling during cell migration. Here we show that expression of Cybr in vivo is differentially modulated by type 1 cytokines during lymphocyte maturation. In mice, Cybr deficiency negatively affects leukocytes circulating in blood and lymphocytes present in the lymph nodes. Moreover, in a Th1-polarized mouse model, lymphocyte trafficking is impaired by loss of Cybr, and Cybr-deficient mice with aseptic peritonitis have fewer cells than controls present in the peritoneal cavity, as well as fewer leukocytes leaving the bloodstream. Mutant mice injected with Moloney murine sarcoma/leukemia virus develop significantly larger tumors than wild-type mice and have reduced lymph node enlargement, suggesting reduced cytotoxic T-lymphocyte migration. Taken together, these data support a role for Cybr in leukocyte trafficking, especially in response to proinflammatory cytokines in stress conditions.

Leukocytes are extremely mobile cells capable of controlling their interactions with other cells or with the extracellular matrix in a fast and efficient manner (25). How the signal received from the extracellular environment is transduced intracellularly to coordinate the appropriate cell response is a major question in leukocyte biology. Scaffold proteins, containing various protein-protein interaction domains, are emerging as molecules able to rapidly integrate signals from different pathways through the interaction with multiple partners, especially in situations of rapid cellular response to an external stimulus (21).

Cybr (also known as B3-1/36.3K zipper-containing protein [8], CBP [12], Cytip [3], and CASP [14]) is a 359-amino-acid (aa) scaffold protein containing two adjacent protein-protein interacting domains: a 90-aa PDZ (postsynaptic density protein-95/discs-large/ZO-1) domain and a 20-aa leucine-rich domain. In particular, the leucine-rich domain is responsible for Cybr interaction with cytohesin-1, a guanine exchange factor (GEF) for the ARF (ADP-ribosylation factors) GTPase family members (3, 27), which have been implicated in cellular vesicular transport and actin cytoskeleton remodeling during cell migration (19, 20, 24).

Cybr is highly expressed in the hematopoietic/immune system. Northern analysis of human RNA shows a main transcript of about 1.3 kb in thymus, spleen, peripheral blood leukocytes (PBLs), lymph node, bone marrow, and lung. In PBLs cultured in vitro, Cybr transcription is up-regulated by cytokines, including interleukin-2 (IL-2) and IL-12 alone or synergistically. IL-18 alone has no effect; however, it synergizes with IL-12 (27).

Cybr interaction with members of the cytohesin family (14, 27) is interesting because of its ability to control ARF function and because the Cybr-cytohesin complex has been shown to regulate LFA-1 (lymphocyte function associated antigen 1)-mediated cell adhesion in T cells. Specifically, Cybr diminishes stimulated adhesion of LFA-1 to intracellular adhesion molecule 1 (ICAM-1) (3). In addition, Cybr regulates T-cell detachment from contact zones with dendritic cells (10). Together, these findings place Cybr in a crucial position to control cell adhesion and trafficking of cells of the immune system.

In order to study the physiological relevance of Cybr function, we have investigated type 1 cytokine modulation of Cybr expression in vivo and the effect of Cybr-targeted deletion in mice. We found that Cybr is expressed at low levels in CD3-negative, less differentiated thymocytes. Stimulation with IL-12 and IL-18 reduces the amount of Cybr transcript in more mature splenic cells. Targeted deletion of Cybr in mice does not seem to affect the development of the immune system, although it does cause a reduction of circulating white blood cells and of lymphocytes present in the lymph nodes of adult animals. Moreover, lack of Cybr causes a deficit in lymphocyte trafficking in the presence of Th1-type cytokines, and in a model of aseptic peritonitis it causes a reduction in the number of cells in the inflamed peritoneal cavity and simultaneously causes fewer leukocytes to leave the blood circulation. To

* Corresponding author. Mailing address: Neural Development Group, Mouse Cancer Genetics Program, National Cancer Institute, Frederick, MD. Phone: (301) 846-1202. Fax: (301) 846-7017. E-mail for Vincenzo Coppola: coppolav@ncifcrf.gov. E-mail for Lino Tessarollo: tessarol@ncifcrf.gov.

investigate its role in the mounting of an immune response to a pathogen, we studied the effect of Cybr deletion in mice injected with Moloney murine sarcoma virus/Moloney murine leukemia virus (MMSV/MuLV, hereafter called M-MSV) retroviral complex. Intramuscular injection of M-MSV causes sarcomas to develop at the inoculation site after a short period of latency. Subsequently, tumors regress because of a strong immune reaction primarily mediated by cytotoxic T lymphocytes (CTL) specific for viral antigens (16). Thus, any change in the animal immune response can be readily quantified based on tumor size and time required for tumor regression. Cybr-deficient mice injected with M-MSV develop larger tumors than controls. In addition, they show a reduction in lymph node enlargement, suggesting that Cybr deficiency negatively affects the number of specific CTL. Taken together, these data provide evidence that Cybr plays a role in trafficking and/or cell adhesion of cells of the immune system.

MATERIALS AND METHODS

Generation of Cybr-deficient mice. The Cybr-specific targeting vector was obtained by recombineering technology (5). Briefly, an 8.8-kb fragment containing Cybr exon 1 (EX1) was retrieved from BAC 265C23 (ResGen; Invitrogen Corp., Huntsville, AL) into the targeting vector. Subsequently, by recombination in the DY380 bacterial strain, a *loxP* site was introduced 83 bp upstream of EX1. Finally, a cassette containing the neo resistance gene flanked by both *loxP* and Frt sites was placed 63 bp downstream of EX1. Cybr mutant mice were generated by a standard gene-targeting approach using the CJ7 embryonic stem cell line as previously described (4, 28). Removal of EX1 was accomplished by crossing the offspring of chimeras with the targeted allele to a Cre deleter strain kindly provided by M. Lewandoski (15). All the mice used in the experimental procedures were backcrossed at least four generations and negatively selected for the presence of Cre. All animals were treated in accordance with the guidelines provided by the Animal Care and Use Committee of the National Cancer Institute at Frederick, MD.

In vivo hydrodynamic delivery of cytokine-encoding DNA. The hydrodynamic gene transfer procedure was conducted as described previously (29). Animals were separated into different groups and injected through the tail vein with the following: 15 μg of empty vector control cDNA; 5 μg of IL-12 cDNA (pscIL-12, p40-p35 fusion gene) plus 10 μg of IL-18 cDNA (pDEF pro-IL-18); IL-12 cDNA alone or IL-18 cDNA alone in 1.6 ml of sterile 0.9% sodium chloride solution. All of the plasmids are driven by human elongation promoter 1-α and were purified using Endofree Mega kits (QIAGEN, Valencia, CA). Mice were injected through their tail vein in a 5-s push using a 27.5-gauge needle at day 0. At different time points mice were bled and euthanized, and then different organs and tissues were collected and processed for single-cell suspension.

Thymocyte and splenocyte isolation. $CD3^-$ and $CD3^+$ thymocytes as well as $CD4^-$ $CD8^-$ $CD3^-$ and $CD4^+$ $CD8^+$ $CD3^+$ spleen cells were separated using magnetic beads (Miltenyi Biotec) according to the manufacturer's instructions. Briefly, following the lysis of red blood cells by hypotonic wash, pooled splenocytes were cultured in plastic flasks for 1 h to obtain adherent cells (macrophage-enriched fraction). The thymocyte suspension and the spleen nonadherent cells were incubated in biotinylated anti-CD3 antibody or in biotinylated anti-CD3, anti-CD4, and anti-CD8 antibodies, respectively, for 30 min at 4°C. Cells were washed, resuspended in 1× phosphate-buffered saline (PBS), and incubated with streptavidin magnetic beads for 15 min at 4°C. Cells were washed again, resuspended in 1× PBS, and eluted in columns to recover the unlabeled negatively selected $CD3^-$ thymocytes or $CD4^-$ $CD8^-$ $CD3^-$ splenocytes (B-cell-enriched fraction). The columns were removed from a magnetic field, and the positively selected $CD3^+$ cell fraction from thymocytes or $CD4^+$ $CD8^+$ $CD3^+$ splenocytes (T-cell-enriched fraction) was collected in 5 ml of 1× PBS.

Northern and RT-PCR analyses. Total RNA was isolated from different tissues and cell suspensions by a single-step phenol-chloroform extraction procedure (RNA STAT-60; Tel-Test "B" Inc., Friendswood, TX) and analyzed by classical Northern blot analysis. Cybr transcripts were detected by using a mouse Cybr full-length-specific probe (spanning EX1 to EX8). Quantization of the amount of Cybr transcript was obtained using IQMac 1.2 (Molecular Dynamics). The results were normalized to the content of cyclophilin transcript. Reverse transcription-PCR (RT-PCR) was performed using SuperScript RT-PCR System (Invitrogen-GIBCO, Gaithersburg, MD) according to the manufacturer's instructions.

Automated blood cell counts were performed using the HEMAVET 850 apparatus (CDC Technologies Inc, Oxford, CT). Data were analyzed and plotted using PRISM 3.0 (GraphPad Software, Inc., San Diego, CA).

Histological procedures. Five-micrometer sections from paraffin-embedded tissues were stained with anti-CD45R (1:200) (B220, RA3-6B2; Pharmingen, San Jose, CA), anti-CD3 (1:600) (Dako, Carpinteria, CA), and anti-mouse F4/80 (1:25) (Caltag, Burlingame, CA) for B-cell-, T-cell-, and macrophage-specific immunostaining, respectively. Apoptotic cells were detected with the Apoptag kit (Intergen, Purchase, NY) following the manufacturer's recommendations.

Flow cytometric analysis. For fluorescence-activated cell sorter (FACS) analysis, samples were prepared as previously described (7). All the unlabeled antibodies, PE (phycoerythrin), fluorescein isothiocyanate, PerCP, and PE-Cy5 conjugated, were purchased from BD Pharmingen (San Jose, CA).

Purification of cells for ex vivo chemotaxis assay. Spleens were aseptically removed and gently disrupted through a cell strainer (pore size, 100 μm; Becton Dickinson) to obtain single-cell suspensions. Erythrocytes were removed by using a Mouse Erythrocyte Lysing kit (R&D Systems, Minneapolis, MN). $CD11b^+$, $CD4^+$, $CD8^+$, and $CD19^+$ cells were enriched by magnetic separation using an MS+ column (Miltenyi Biotech, Auburn, CA). Cells were then resuspended in chemotaxis medium (RPMI 1640 medium containing 1% bovine serum albumin, 25 mM HEPES, pH 8.0) at 1×10^6 to 5×10^6 cells/ml. Chemokines, including RANTES, SDF-1α (stromal derived factor 1α), SLC (secondary lymphoid tissue chemokine), BCA (B-cell-attracting chemokine 1), MCP-5 (macrophage chemoattractant protein 5), and JE, were diluted in chemotaxis medium and placed in the lower wells of a micro-Boyden chemotaxis chamber (Neuro Probe, Gaithersburg, MD). Five-micrometer polycarbonate membranes were placed over the chemokines. Detection of lymphocyte chemotaxis required that the membranes be precoated with 50 μg/ml of fibronectin. After the microchemotaxis chamber was assembled, 50 μl of cells was placed in the upper wells. The filled chemotaxis chambers were incubated in a humidified CO_2 incubator for 60 min ($CD11b^+$) or 3 h (lymphocytes). After incubation, the membranes were removed from the chemotaxis chamber assembly followed by gently removing cells from the upper side of the membrane. The cells on the lower side of the membrane were stained using a Rapid Stain kit (Richard Allen, Kalamazoo, MI). The number of migrated cells in three high-powered fields (×200) was counted by light microscopy after coding the samples. Quantitation of mouse cell chemotaxis was computer assisted using the BIOQUANT program (R & M Biometrics, Nashville, TN). Results are expressed as the mean value of the migration of triplicate samples with the standard errors shown by bars. Chemotactic indices were calculated as follows: (mean number of migrating cells in sample)/(mean number of cells in media control).

Adoptive transfer of CFSE-labeled lymphocytes. Single-cell suspensions were obtained from spleens of donor female wild-type (WT) and Cybr null mice. Splenocytes were then labeled with 5,6-carboxyfluorescein diacetate (CFSE) as previously described (2). A total of 10×10^6 lymphocytes were injected into the tail vein of recipient C57BL/6 females. In different experiments, cells were subjected to enrichment for a specific population before labeling and injection. For enrichment purposes, Spin Sep negative selection kits for B and T cells from Stem Cell Technologies (Vancouver, Canada) were used. Recipient females were sacrificed in most of the experiments 1 h after the injection (11). However, a time course experiment was performed at different time points from 15 min up to 150 min after injection.

Aseptic peritonitis induction. Aseptic peritonitis was induced by intraperitoneal injection of 0.5 ml of pristane (2,6,10,14-tetramethylpentadecane; Sigma), and peritoneal cells were recovered as previously described (6). Briefly, at 6 or 7 days postinjection, mice were euthanized by CO_2 asphyxiation, and then inflammatory cells were harvested by washing the peritoneal cavity with 10 ml of ice-cold PBS–1% bovine serum albumin and immediately processed for FACS analysis.

M-MSV retroviral complex preparation and tumor induction. Tumor cell extract containing defective M-MSV (Moloney murine sarcoma virus copelleted with its natural helper, Moloney murine leukemia virus) was prepared from primary sarcomas induced by serial passages in 1-week-old BALB/c mice. M-MSV extract had an in vitro titer of 5×10^5 focus-forming units/ml on 3T3/FL cells. Aliquots of 0.15 ml of M-MSV extract were injected intramuscularly in the thigh region of adult mice. Tumor growth was monitored daily by caliper measurement starting 5 days after inoculation, when sarcomas become apparent (22, 23).

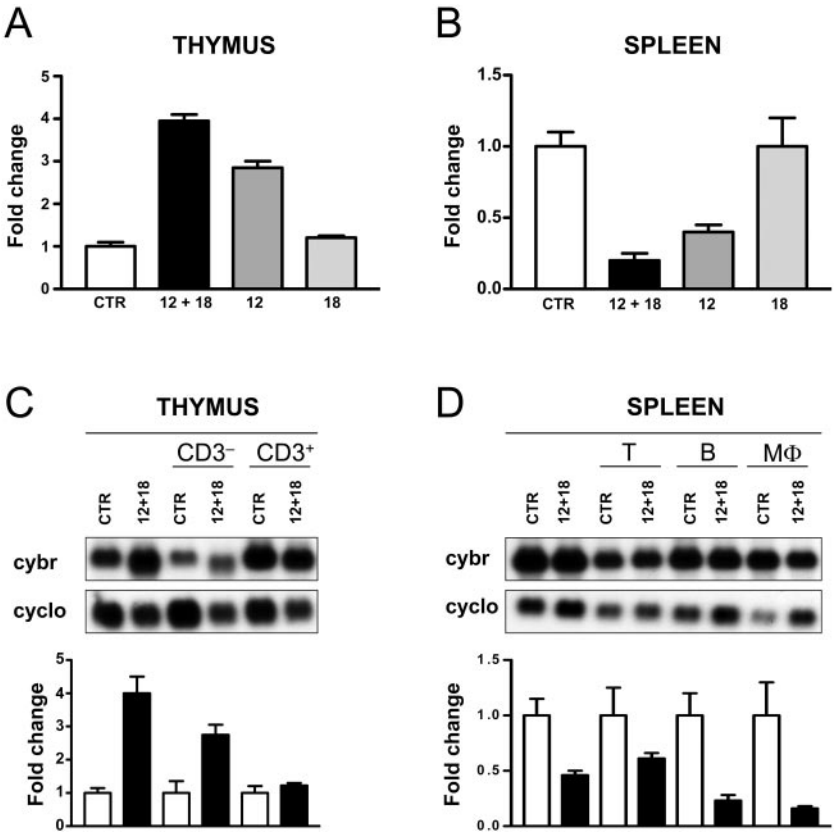

FIG. 1. In vivo analysis of Cybr gene expression. (A) Th1 cytokines increase Cybr expression in thymus. Quantitation of Northern blots from RNA obtained from thymus of C57BL/6 mice 96 h after intravenous injection of a cDNA encoding IL-12, IL-18, or both (12 + 18). The empty vector was injected in animals and used as a control (CTR). In each experiment, two mice were used. Expression of the ~2.0-kb Cybr-specific transcript is quantified relative to housekeeping cyclophilin (cyclo) gene expression. Results are representative of at least three separate experiments. (B) Th1 cytokines reduce Cybr expression in spleen. RNA derived from splenocytes obtained from the same animals used for thymocyte analysis was obtained and analyzed as described for panel A. (C and D) Cybr expression in different thymus (C) and spleen (D) cell populations in response to cytokines. $CD3^-$ and $CD3^+$ thymocytes were obtained from the thymus of CTR- or IL-12 cDNA- and IL-18 cDNA-injected mice. The spleens from the same mice were harvested to obtain B-cell ($CD19^+$)-, T-cell ($CD3^+$)-, or MΦ ($CD11b^+$)-enriched populations. Specific cell population enrichment was performed as described in Materials and Methods and was verified by FACS analysis as more than 90%.

RESULTS

Cybr expression is differentially regulated by cytokines at different stages of T-lymphocyte development. IL-12 synergizes with IL-2 and IL-18 to increase Cybr expression in human PBLs (27). However, virtually nothing is known of the effect of cytokines on Cybr expression in vivo. By Northern blot analysis of mouse tissue RNA, we confirmed that Cybr is mostly expressed in organs of the immune system, such as spleen, thymus, bone marrow, and lymph nodes, as reported for humans (27 and data not shown). Other organs in which Cybr transcripts are detectable at lower levels are lung, kidney, and testis (data not shown). Next, we sought to determine if Cybr expression in mice is increased by proinflammatory type 1 cytokines such as IL-12 in combination with IL-18, as reported for human PBLs. For this, we employed an in vivo hydrodynamic delivery of cDNA encoding IL-12 alone or the combination of IL-12 and IL-18 (29). In thymocytes, IL-12 alone enhanced Cybr expression by two- to threefold, and addition of IL-18 synergistically increases Cybr expression up to fourfold after 96 h from the treatment of the animal. IL-18 alone had no effect, as reported for humans (Fig. 1A). Thus, IL-12 and IL-18 act in vivo as reported for human PBLs in vitro. Surprisingly, RNA analysis from the same animals shows that the same cytokines down-regulate Cybr expression in splenocytes (Fig. 1B). Again, IL-12 synergizes with IL-18 and causes a Cybr expression reduction of about 80%. IL-12 alone reduces Cybr levels to about 50%, while IL-18 has no effect. To exclude the possibility that the Cybr expression changes observed in thymus and spleen were due to a shift in cell composition of those organs caused by cytokine treatment, we studied the individual cell populations including enriched $CD3^-$ or $CD3^+$ thymocytes (Fig. 1C), macrophages (MΦ), and T and B lymphocytes from spleen (Fig. 1D). In the thymus, less differentiated $CD3^-$ T cells show a lower expression level of Cybr compared to the $CD3^+$ fraction. However, upon stimulation with IL-12 and IL-18, the $CD3^-$ T cells respond by significantly up-regulating Cybr mRNA, while the mature $CD3^+$ T cells do not show any significant response. In general, splenocytes have relatively high basal levels of Cybr expression, and following cytokine treatment, all cell populations, including the T lymphocytes,

decrease the amount of Cybr message. Taken together, our data indicate that in T cells, Cybr is up- or down-regulated in response to cytokine stimulation depending on their differentiation stage. Moreover, our results suggest that Cybr may play a role in lymphocyte function in response to proinflammatory cytokines.

Generation of Cybr knockout mice. To investigate Cybr's role in vivo, we generated a Cybr-deficient mouse by gene targeting deletion. We used recombineering technology to construct a vector to conditionally inactivate Cybr (5). As described in Materials and Methods, we flanked the first coding exon (EX1) with *loxP* sites because it contains the ATG starting codon (Fig. 2A). Correct targeting of Cybr in ES cells was confirmed by Southern analysis both at the 5′ and 3′ ends (data not shown). Deletion of Cybr EX1 was accomplished in vivo by crossing the Cybr targeted mouse line with a Cre deleter strain (15) (Fig. 2B). To investigate whether deletion of EX1 was sufficient to generate a Cybr null allele and no truncated proteins were made, we raised an antibody against the Cybr carboxy terminus, which is downstream of EX1. Western blot analysis of Cybr knockout (KO) splenocytes with the anti-Cybr antibody shows that no Cybr-specific protein is produced in the mutant mice (Fig. 2C). Moreover, deletion of one allele causes a ~50% reduction of Cybr, suggesting that two intact alleles are required to have normal Cybr protein levels in vivo.

Cybr-deficient mice have reduced numbers of lymphocytes present in the lymph nodes and leukocytes circulating in blood. Cybr-deficient mice are viable and are born at the expected Mendelian ratio. They appear normal and are fertile. Since the highest level of Cybr expression is in lymphoid organs, we stained sections from thymus, spleen, and lymph nodes with anti-CD45R (for B cells), anti-CD3 (T cell specific), and anti-mouse F4/80 (for macrophages) to look for the presence and distribution of the major cell populations in these organs. In the absence of Cybr, we could not detect any obvious histological abnormality or any difference in the number of apoptotic cells in lymphoid organs (data not shown). Furthermore, flow cytometric analysis of lymphoid organs using antibodies specific to B and T lymphocytes and macrophages did not reveal any significant difference in mutant animals compared to controls (data not shown). However, we did find that Cybr-deficient mice older than 6 months have significant reductions in the numbers of circulating white blood cells (WBC) and lymphocytes in the inguinal lymph nodes (Table 1). WBC deficits were almost entirely caused by a decrease in circulating lymphocytes and secondarily by a reduction in the neutrophilic and monocytic fractions (data not shown). Flow cytometric analysis of circulating leukocytes did not reveal a specific reduction in T, B, or Gr-1- and Mac-1-positive cells. Likewise, flow cytometric analysis of inguinal lymph nodes from adult Cybr-deficient mice shows that the reduction affects both T and B lymphocytes (data not shown). Analysis of other immune system organs or districts including thymus, spleen, bone marrow, and the peritoneal cavity does not show any other apparent deficits (Table 1). Taken together, these results suggest that Cybr deficiency affects recirculation of blood leukocytes and peripheral lymph node lymphocytes.

Abnormal trafficking of Cybr$^{-/-}$ lymphocytes in vivo. LFA-1-deficient mice show migration deficits (1, 2). Since Cybr has been shown to regulate LFA-1 function (3) and we have observed reductions of circulating WBC and lymph node lymphocytes, we investigated whether Cybr-deficient mice have abnormalities in leukocyte migration. We first analyzed whether Cybr deficiency could affect cell migration by using a classic in vitro chemotaxis assay. CD4$^+$, CD8$^+$, CD19$^+$, and CD11b$^+$ splenic cells were separated as described in Materials and Methods and treated with a variety of chemokines known to induce migration (Fig. 3A). In general, none of the isolated

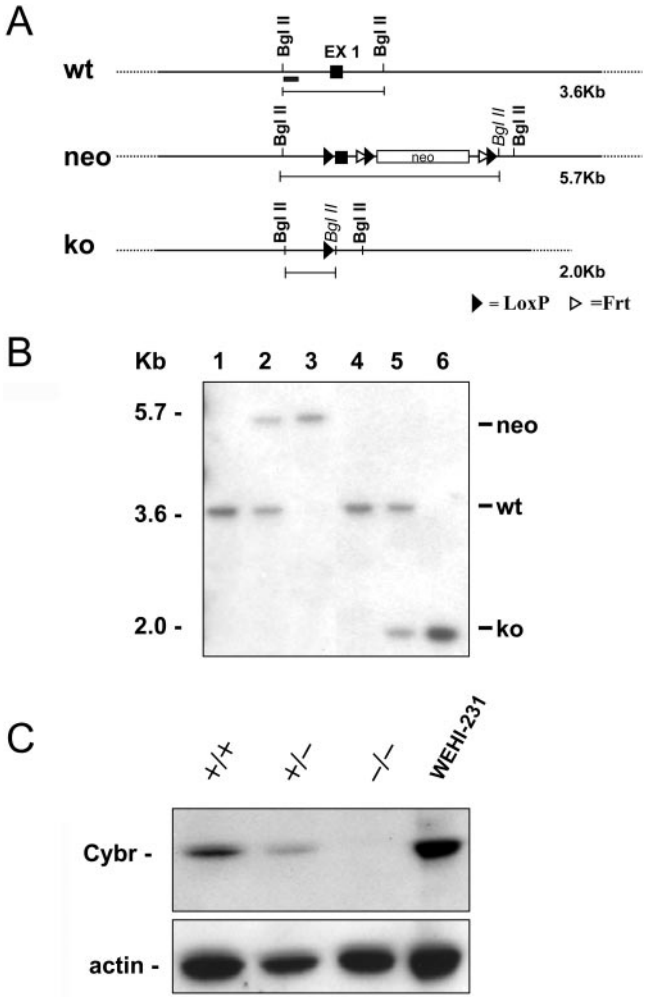

FIG. 2. Generation of Cybr mutant mice. (A) Gene targeting strategy to delete Cybr exon 1 (EX1). *loxP* sites (black triangles) were inserted upstream and downstream of EX1. The neomycin resistance cassette is flanked by both *loxP* and Frt (white triangle) sites. After the initial screening of the positive ES cell clones, as described in Material and Methods, a probe upstream of EX1 (black rectangle) was used for the identification of the different targeted alleles. (B) Southern analysis of genomic DNA from Cybr mutant mice. Analysis of DNA digested with the BglII restriction enzyme and probed with the 5′ fragment described for panel A yields the expected 3.6-kb band in a wild-type mouse (wt) (lanes 1 and 4) and a rearranged 5.7-kb fragment with the neo insertion (neo) in heterozygous and mutant mice (lanes 2 and 3, respectively). Following EX1 cre excision, the same probe detects a 2-kb band corresponding to the null allele (ko) (lanes 5 and 6). (C) Western blot analysis of lysates from splenocytes of wild-type (+/+), heterozygote (+/−), and Cybr null (−/−) mice. Using an antibody specific to the COOH terminus, Cybr is undetectable in null mice. Lysate from the WEHI-231 B-cell line was used as positive control.

TABLE 1. Cell counts in different organs and tissues of the immune system of Cybr-deficient mice[a]

Mouse type	WBC (10^3 cells/μl)	Thymus[b]	Spleen[b]	Bone marrow[b,c]	Inguinal lymph nodes[b]	Peritoneal cells[b]
WT	9.98 ± 0.87	93.40 ± 5.68	55.61 ± 10.14	35.35 ± 2.06	3.68 ± 1.04	2.11 ± 0.46
KO	7.52 ± 1.15	96.56 ± 17.72	62.07 ± 11.01	34.25 ± 2.36	2.04 ± 0.43	2.50 ± 0.63
P value	0.0018	NS	NS	NS	0.0347	NS

[a] Each analysis includes at least six mice. KO, Cybr deficient. *P* values were obtained by Student *t* test analysis of the data. NS, not significant.
[b] Total number of cells (in millions).
[c] Total numbers from cell counts of two femurs.

mutant cell populations showed significant migration abnormalities in response to the tested chemokines compared to wild-type control cells (Fig. 3A). Only mild reductions in migration were noted for mutant B cells treated with SDF-1α (CXCL12) and SLC (CCL21). These data suggest that either Cybr does not affect the migration pathways activated by the specific chemokines used in our assay or our test does not reflect the more complex in vivo scenario. Therefore, we decided to test the trafficking efficiency of Cybr-deficient leukocytes in vivo by adoptive transfer in C57BL/6 mice. Splenic single-cell suspensions were labeled with CFSE, as described above (2). In one set of experiments, nonfractionated splenocytes inoculated by tail vein injection were recovered from the host after 1 h to see whether Cybr KO cells showed any anomaly in short-term migration to different organs (Fig. 3B). Only nonsignificant differences were noted in percentages and absolute numbers of CFSE-labeled mutant cells from different groups found in peripheral blood, spleen, and inguinal lymph nodes (Fig. 3B). Similar results were obtained in time course experiments in which cells were harvested at different time points, ranging from 15 to 150 min after tail vein injection (data not shown). Since nonfractionated Cybr-deficient splenocytes injected into C57BL/6 recipients did show small yet nonsignificant abnormalities in their recirculation ability, we investigated whether specific subpopulations were impacted more significantly by the Cybr mutation. Splenic CFSE-labeled T and B lymphocytes were injected into recipient C57BL/6 mice and recovered after 1 h. Again, no differences were found in trafficking of either Cybr-deficient T (Fig. 3C) or B (Fig. 3D) lymphocytes compared to wild-type lymphocytes. This lack of a clear cell migration deficit was somewhat surprising in light of the fact that Cybr has been reported to regulate LFA-1 binding capacity, which is crucial for immune system cell trafficking and recirculation in vivo (3).

Since Cybr expression is influenced by Th1-type cytokines and might therefore affect cell migration ability after cytokine stimulation, we next decided to assess the effect of Cybr deficiency on cell trafficking in an in vivo system in which cytokines are overexpressed. C57BL/6 recipient animals were preinjected with a mixture of IL-12- and IL-18-encoding cDNA. After 24 h, the recipient mice were injected with CFSE-labeled splenocytes from WT or Cybr null animals. Organs were collected and analyzed for the presence of the labeled splenocytes after 1 h as in the previous experiment. We found that in this in vivo experimental paradigm, splenocytes from Cybr-deficient mice were less efficient in migrating to the spleen, suggesting a Cybr role in lymphocyte trafficking in Th1-polarized conditions (Fig. 3E).

Deficient recruitment of Cybr$^{-/-}$ inflammatory cells to the peritoneal cavity in an aseptic peritonitis model. We have found that in vivo Cybr expression is modulated by proinflammatory cytokines (Fig. 1). Furthermore, LFA-1 has been shown to have a crucial role in cell adhesion and migration during inflammation (18). Thus, we decided to induce aseptic peritonitis by injecting 0.5 ml of pristane in the peritoneal cavity of Cybr wild-type and mutant animals and assess the presence of inflammatory cells. Blood was collected 7 days before pristane treatment as a control. Seven days after the pristane injection, mice were bled again and immediately sacrificed to harvest the peritoneal cells. As shown in Fig. 4A, Cybr KO mice had a significantly lower number of peritoneal inflammatory cells than the wild-type controls ($22.53 \times 10^6 \pm 3.80 \times 10^6$ versus $29.91 \times 10^6 \pm 3.85 \times 10^6$). FACS analysis showed that this reduction was generalized to all cell types. In fact, Cybr-deficient mice had lower numbers of peritoneal $CD4^+$ and $CD8^+$ T lymphocytes, B cells, Mac-1^+/Gr-1^+ MΦ cells (Fig. 4B), and Mac-1^+ and Gr-1^+ cells (data not shown). Interestingly, the change in cell counts from before the induction of inflammation to the day of inflammatory cell collection was different in the peripheral blood of Cybr KO mice from that of wild-type littermates (Fig. 4C). In fact, Cybr KO mice had a smaller number of WBC before the pristane injection than wild-type controls ($7.764 \times 10^3/\mu l \pm 1.09 \times 10^3/\mu l$ versus $9.740 \times 10^3/\mu l \pm 0.71 \times 10^3/\mu l$; Fig. 4C); however, after peritonitis induction, Cybr mutant mice showed only a limited decrease in the number of circulating WBC, while wild-type control animals had an almost 50% reduction caused by peritoneal inflammation (Fig. 4C). Moreover, WBC differential count analysis showed that the observed differences might mostly be due to neutrophils failing to efficiently exit the bloodstream, since they are present in greater numbers in the circulation of Cybr KO mice ($1.922 \times 10^3/\mu l \pm 0.3884 \times 10^3/\mu l$ versus $1.332 \times 10^3/\mu l \pm 0.1425 \times 10^3/\mu l$; Fig. 4D, bottom right panel). These results suggest that the cells recirculating to the inflamed peritoneal cavity are affected by the lack of Cybr.

Cybr deficiency enhances M-MSV-induced tumor growth in vivo. The above data suggest a function for Cybr in the recirculation of cells of the immune system (Fig. 4). To test whether Cybr affects the response of antigen-specific T lymphocytes to a pathogenic microorganism infecting the host in a specific location, we studied the growth of M-MSV-induced tumors in Cybr-deficient mice. In this model, intramuscular injection of M-MSV causes sarcomas to develop at the inoculation site after a short period of latency. Subsequently, tumors regress because of a strong immune reaction primarily mediated by CTL specific for viral antigens (16). Cybr mutant mice injected

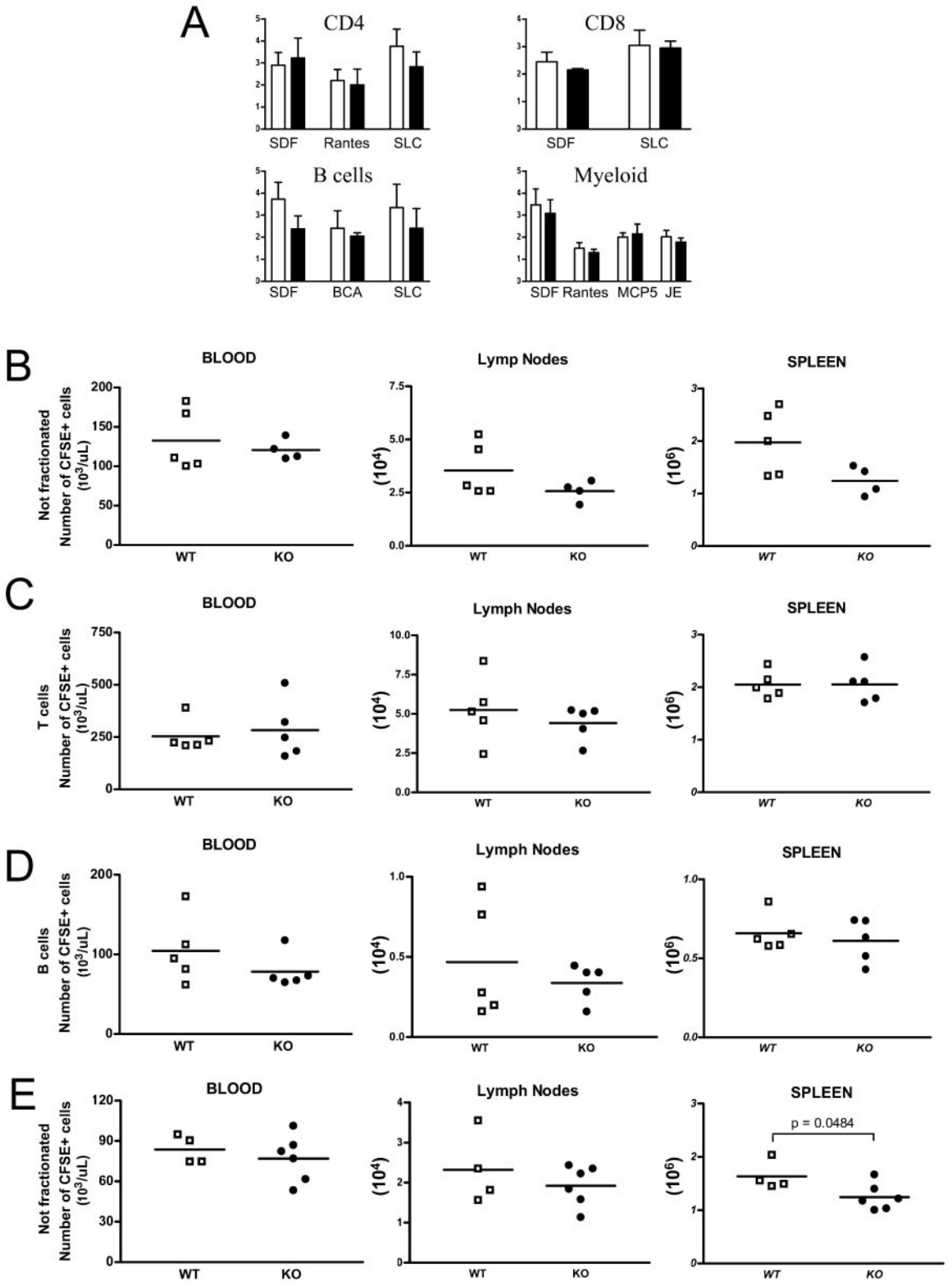

FIG. 3. Ex vivo chemotaxis response and adoptive transfer of Cybr-deficient splenocytes. (A) Ex vivo chemotaxis response is not impaired in $CD4^+$, $CD8^+$, $CD19^+$ (B cells), and myeloid ($CD11b^+$) cells. Cells were enriched by magnetic separation from spleen single-cell suspensions and tested for their migratory capacity in micro-Boyden chambers in response to different factors (SDF, Rantes, MCP, SLC, and BCA). Chemotactic indices for wild-type (open bars) and Cybr-deficient (black bars) cells were calculated with the following formula: (mean number of migrating cells in sample)/(mean number of cells in media control). Results are expressed as the mean value of the migration of triplicate samples plus or minus the standard errors of the means. (B, C, and D) Circulation of wild-type (WT) and mutant (KO) CFSE-labeled nonfractionated splenocytes (B), enriched T cells from spleen (C), and enriched B cells from spleen in blood, lymph nodes, and spleen (D). Note that Cybr KO nonfractionated

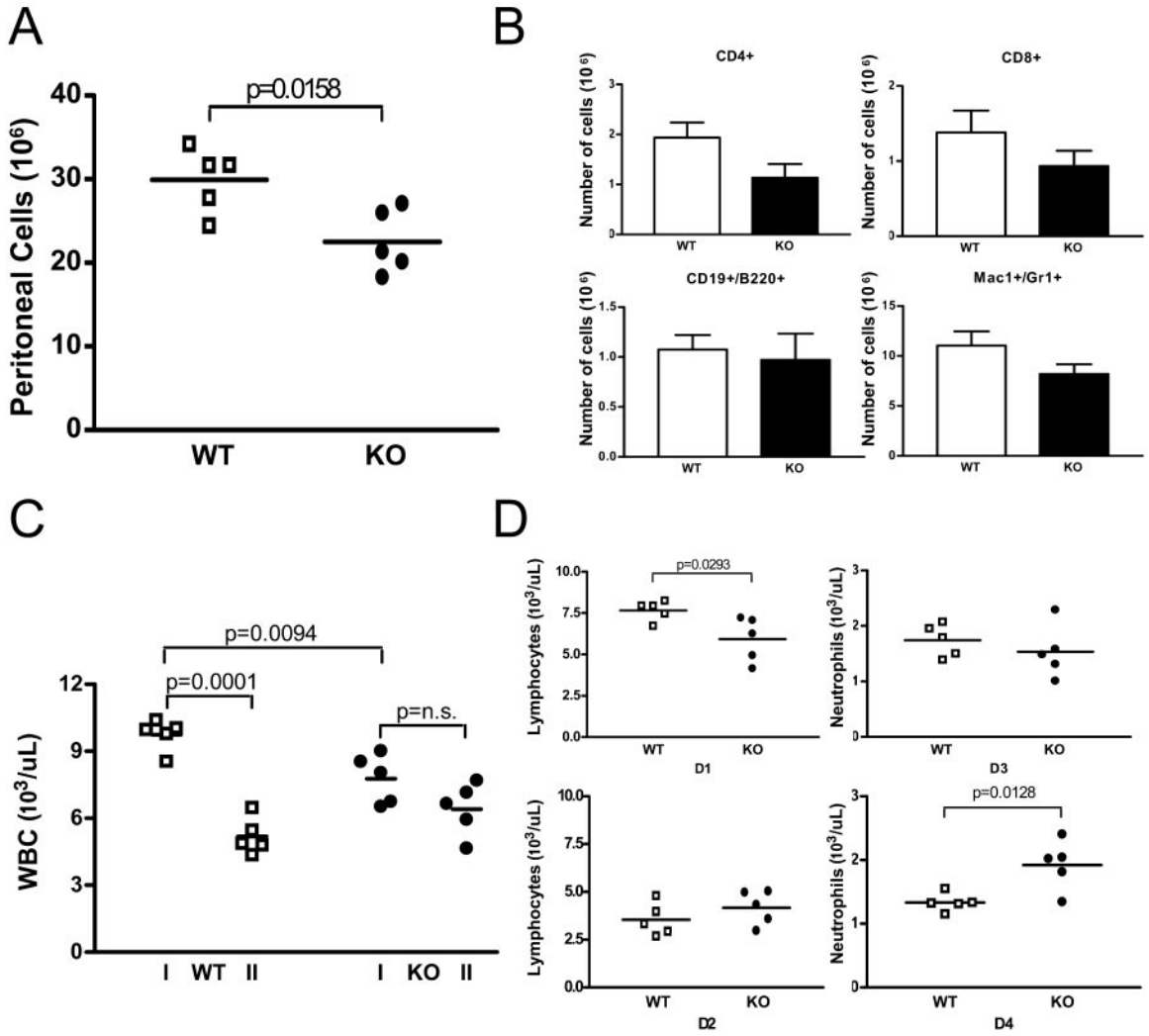

FIG. 4. Analysis of inflammatory response by Cybr-deficient mice in a model of aseptic peritonitis. (A) Cybr-deficient and wild-type mice 7 days after the control bleeding were injected intraperitoneally with 0.5 ml of pristane to induce peritoneal inflammation. After 7 additional days, mice were bled and sacrificed to harvest cells by washing the peritoneal cavity with 10 ml of ice-cold PBS–3% bovine serum albumin. Cybr-deficient mice showed a significantly smaller number of cells present in the peritoneal cavity after inflammation ($21.94 \times 10^6 \pm 3.7 \times 10^6$ versus $29.13 \times 10^6 \pm 3.9 \times 10^6$). (B) Cytofluorimetric analysis of inflammatory cells from the peritoneal cavity shows that T cells ($CD4^+$ and $CD8^+$), B ($CD19^+$) cells, and MΦ ($Mac1^+/Gr1^+$) are all reduced in Cybr KO mice compared to wild-type controls. (C) Cybr-deficient mice before injection (I) showed fewer WBC ($9.98 \times 10^3/\mu l \pm 0.87 \times 10^3/\mu l$ versus $7.52 \times 10^3/\mu l \pm 1.15 \times 10^3/\mu l$; $n = 5$). However, 1 week after pristane injection (II), WBC expressed as percentages of initial WBC present 7 days before the peritonitis induction are significantly higher in Cybr-deficient mice than in wild-type controls (77.06% ± 15.29% versus 59.13% ± 16.48%; data not shown). (D) At the time of sacrifice, after induction of inflammation (panels D2 and D4), Cybr-deficient mice had a significantly larger number of neutrophils circulating in the bloodstream ($1.922 \times 10^3/\mu l \pm 0.3884 \times 10^3/\mu l$ versus $1.332 \times 10^3/\mu l \pm 0.1425 \times 10^3/\mu l$; D4 versus D3) compared to the preinflammatory state (panels D1 and D3), while lymphocytes (D2 versus D1) and monocytes (not shown) were not significantly different.

with M-MSV exhibited a higher, although nonsignificant, level of tumor incidence than wild-type controls (20/23 [87%] versus 14/20 [70%], respectively). Notably, tumor-bearing Cybr KO mice developed significantly larger sarcomas than wild-type mice (Fig. 5A). Although most animals were sacrificed at day 13 from the injection to analyze spleen and lymph node cellularity, in a group of animals ($n = 5$) in which tumor growth was monitored for up to 1 month, sarcomas ultimately regressed

splenocytes and T cells and B cells enriched from spleen showed percentages (data not shown) and absolute numbers of $CFSE^+$ cells comparable to those of the wild type circulating in the periphery or migrated to the inguinal lymph nodes and spleen of nontreated recipients 1 h after inoculation. (E) When recipient animals are preinjected with a mixture of IL-12- and IL-18-encoding cDNA, 24 h prior the intravenous injection of labeled cells, Cybr KO $CFSE^+$ splenocytes show a small but significant deficit in recirculation to spleen, while numbers of $CFSE^+$ Cybr KO cells are comparable to those of wild-type cells in blood and inguinal lymph nodes.

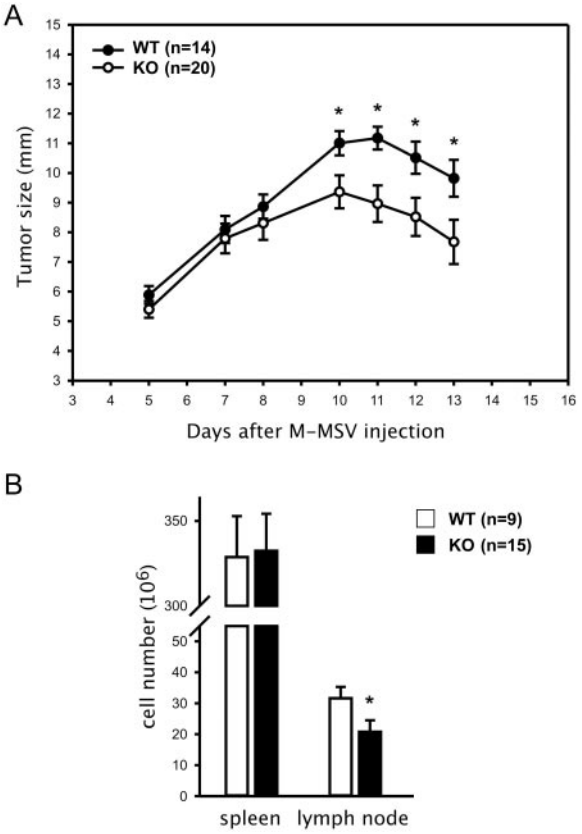

FIG. 5. Analysis of M-MSV-induced tumor growth in Cybr-deficient mice. (A) Cumulative kinetics of tumor growth in Cybr knockout (filled circles) and wild-type control littermates (open circles) from three different experiments are shown. Twenty out of 23 (86.9%) Cybr-deficient and 14 out of 20 (70.0%) wild-type mice injected intramuscularly with M-MSV developed sarcomas. Tumor size (in milimeters) was monitored up to day 13, when most of animals were sacrificed. *, $P < 0.05$ (Student t test). (B) Total number of cells in spleen and tumor-draining lymph node of tumor-bearing mice at day 13 from the M-MSV inoculation. *, $P < 0.05$ (Mann-Whitney U test).

with slower kinetics than those of controls (data not shown). Moreover, the numbers of lymphocytes accumulating in tumor-draining lymph nodes of Cybr-deficient mice were significantly reduced compared to those present in control mice ($20.8 \times 10^6 \pm 14.4 \times 10^6$ versus $31.6 \times 10^6 \pm 11.2 \times 10^6$; $P = 0.0148$, Mann-Whitney U test; Fig. 5B), while splenocyte numbers were not significantly different between the two groups of mice ($332.4 \times 10^6 \pm 84.4 \times 10^6$ in mutants versus $328.7 \times 10^6 \pm 72.4 \times 10^6$ in controls; Fig. 5B). In addition, preliminary data suggest that there are fewer leukocytes infiltrating the tumors as well as reduced numbers of virus-specific CTL in Cybr KO mice compared to wild-type mice (data not shown). Taken together, these results indicate that Cybr deficiency has a significant impact on antigen-specific immune responses. Interestingly, the finding that Cybr deficiency affects lymphocyte accumulation in tumor-draining lymph nodes and recruitment to the neoplastic site is consistent with the decrease in the number of cells observed in the inflamed peritoneal cavity of the aseptic peritonitis model.

DISCUSSION

Cybr is an intracellular scaffold protein that has been implicated in intercellular adhesion of lymphoid cells by regulating integrin deactivation and cytoskeletal rearrangements (3, 27). Most Cybr functions have been attributed to its interaction with cytohesin-1, a GEF for the ARF GTPases, that affects cell ruffling and regulates cell adhesion through its association with integrins (9). Indeed, in vitro studies have shown that Cybr interaction with cytohesin causes a down-modulation of LFA-1-mediated stimulated adhesion in T lymphocytes (3) and T-cell detachment from dendritic cells (10). Such in vitro roles are supported by the wide expression of Cybr as well as of LFA-1 (2, 13) and cytohesins (30) in different populations of the immune system. Nevertheless, virtually nothing is known about Cybr function in vivo.

In this study, we report that Cybr expression in the murine thymus is increased by IL-12 alone or synergistically with IL-18, confirming similar findings for human PBLs. Surprisingly, we found that splenocytes respond in an opposite way to the same cytokines by down-modulating Cybr message. In standard pathogen-free housing conditions, Cybr-deficient mice show a limited reduction in the number of circulating blood leukocytes and peripheral lymph node lymphocytes. Our analysis suggests that this phenotype could be caused by trafficking abnormalities. In fact, Cybr-deficient splenocytes show impaired migration to the spleen of Th1-polarized hosts by expression of proinflammatory type 1 cytokines. In addition, in an aseptic peritonitis model, Cybr-deficient mice have fewer inflammatory cells in the peritoneal cavity associated with reduced numbers of leukocytes exiting the bloodstream. Lastly, Cybr-deficient mice are less efficient in eliminating virus-induced sarcomas and have fewer cells in the draining lymph nodes, as well as fewer lymphocytes infiltrating the tumor.

We have found that $CD3^-$, less differentiated thymocytes have a much lower level of expression of Cybr than the more differentiated $CD3^+$ cells. However, less differentiated cells respond to cytokines by increasing Cybr expression (Fig. 2C), while more mature cells do not show any significant change in its expression. Interestingly, all major cell populations of the spleen, including MΦ and B and T lymphocytes, down-regulate Cybr expression in response to IL-12 plus IL-18 (Fig. 1D). Thus, it appears that cytokines induce Cybr expression in differentiating T lymphocytes, but afterward more mature T cells present in the spleen respond to cytokines, decreasing the amount of cellular Cybr. These results are in agreement with data obtained from dendritic cells where Cybr transcripts increase significantly during in vitro induction of cell maturation (3, 10). Therefore, it is conceivable that, while Cybr may be required but not necessary during the early cellular differentiation stages, more mature cells must lower the amount of Cybr for proper response to cytokines (see below).

Cybr deficiency does not appear to significantly influence in vitro chemotaxis of resting lymphocytes. In fact, splenocytes from Cybr KO mice ex vivo respond to chemoattractant stimuli without significant differences compared to WT cells in a classic micro-Boyden chamber system (Fig. 3A). However, in stress conditions caused by overexpression of proinflammatory type 1 cytokines or induction of peritoneal inflammation, Cybr-deficient mice show significant differences in cell migration com-

pared to wild-type littermate controls. The different outcome observed when Cybr is absent in an in vitro versus an in vivo experimental system is somehow similar to that of LFA-1-deficient cells. In fact, in vitro LFA-1-deficient T lymphocytes migrate as efficiently as wild-type T cells along a gradient of STCP-1 (CCL22) across fibronectin-coated inserts. However, they are impaired in migrating through brain endothelial cells (1). In addition, LFA-1-deficient mice exhibit reduced lymph node cellularity and splenomegaly, consistent with a major role of LFA-1 in normal lymphocyte recirculation (1, 2, 26).

In an aseptic peritonitis model, we have found that Cybr deficiency affects the recirculation of immune system cells to the inflamed peritoneal cavity. Since this phenotype does not reflect the impact of Cybr deficiency on an adaptive specific immune response, we employed the M-MSV-induced sarcoma paradigm. Injections of Cybr mutant mice with the M-MSV retrovirus complex induce the development of significantly larger sarcomas and accumulation of fewer lymphocytes in tumor-draining lymph nodes than wild-type controls. Thus, loss of Cybr impairs the immune response to a pathogen infection. Interestingly, the M-MSV-induced tumor phenotype observed in Cybr mutant mice closely resembles previous findings showing that systemic administration of an anti-LFA-1 monoclonal antibody alone or in combination with an anti-ICAM-1 monoclonal antibody enhances the growth of tumors induced by M-MSV in mice and prevents lymph node hyperplasia (22, 23). M-MSV-induced tumor regression is caused by a strong T-cell-mediated immune reaction leading to the generation of CTL which eliminate cells transformed by the virus (16). In this model, the tumor site is highly inflammatory, and cytokines such as gamma interferon, which is induced by IL-12, play a fundamental role in CTL induction (31). Cybr deficiency might affect different phases of the immune response to M-MSV, including (i) T-cell interaction with the endothelium during migration to secondary lymphoid organs and the tumor site, (ii) T-cell sensitization by tumor antigens or antigen-presenting cells, and (iii) effector CTL adhesion to the tumor cells and subsequent destruction. While we cannot rule out these last two scenarios, the lower cell accumulation and recruitment in reactive lymph nodes and tumors suggests that Cybr deficiency negatively affects lymphocyte recirculation and reduces the extravasation of leukocytes recruited by inflammatory cytokines released at the tumor site. Further investigations will help to determine which phase(s) of the immune response is most critically affected by Cybr.

In nonstress conditions, Cybr-deficient mice do not show any overt phenotype except for some abnormalities in peripheral blood and lymph nodes (Table 1). Since Cybr has been shown to down-regulate LFA-1 affinity/avidity, decreasing stimulated adhesion of T lymphocytes to ICAM-1 (3), our data suggest that most likely Cybr is not a unique player in the important function of attenuating LFA-1 activation. The lack of more dramatic developmental phenotypes suggests that Cybr-activated pathways may be controlled by other similar scaffold proteins. Indeed, Cybr has significant homology with the scaffold protein Tamalin (also known as Grasp, for Grp-1-associated scaffold protein). They share about 74% similarity (~55% identity) at the PDZ domain, and most importantly, their leucine-rich domains, which interact with cytohesins, are 65% identical (~90% similar). While Tamalin is expressed preferentially in brain, lung, and heart (12, 17, 27), it is also expressed at lower levels in spleen and thymus (V. Coppola and L. Tessarollo, unpublished observation). Thus, it is possible that even low levels of Tamalin expression can compensate for Cybr deficiency. The generation of Tamalin-deficient mice and consequently double mutants for both Tamalin and Cybr may help address whether these genes have overlapping developmental functions in vivo.

ACKNOWLEDGMENTS

We thank Daniel McVicar, Debbie Hodge, and Franca Aiello for helpful discussions and critical review of the manuscript, John Wine for his technical assistance with the tail vein injections, Roberta Smith, Leslie Johnston, and Keith Rogers at the PHL, SAIC, Frederick, Md., for the histological analysis, Susan Reid and Eileen Southon for ES cell manipulations and blastocyst injections, and Hui-Fang Dong for isolation of the cells used in the chemotaxis studies.

This research was supported by the Intramural Research Program of the NIH, National Cancer Institute, Center for Cancer Research.

REFERENCES

1. **Andrew, D. P., J. P. Spellberg, H. Takimoto, R. Schmits, T. W. Mak, and M. M. Zukowski.** 1998. Transendothelial migration and trafficking of leukocytes in LFA-1-deficient mice. Eur. J. Immunol. **28:**1959–1969.
2. **Berlin-Rufenach, C., F. Otto, M. Mathies, J. Westermann, M. J. Owen, A. Hamann, and N. Hogg.** 1999. Lymphocyte migration in lymphocyte function-associated antigen (LFA)-1-deficient mice. J. Exp. Med. **189:**1467–1478.
3. **Boehm, T., S. Hofer, P. Winklehner, B. Kellersch, C. Geiger, A. Trockenbacher, S. Neyer, H. Fiegl, S. Ebner, L. Ivarsson, R. Schneider, E. Kremmer, C. Heufler, and W. Kolanus.** 2003. Attenuation of cell adhesion in lymphocytes is regulated by CYTIP, a protein which mediates signal complex sequestration. EMBO J. **22:**1014–1024.
4. **Bonin, A., S. W. Reid, and L. Tessarollo.** 2001. Isolation, microinjection, and transfer of mouse blastocysts. Methods Mol. Biol. **158:**121–134.
5. **Copeland, N. G., N. A. Jenkins, and D. L. Court.** 2001. Recombineering: a powerful new tool for mouse functional genomics. Nat. Rev. Genet. **2:**769–779.
6. **Coppola, V., C. A. Barrick, E. A. Southon, A. Celeste, K. Wang, B. Chen, B. Haddad El, J. Yin, A. Nussenzweig, A. Subramaniam, and L. Tessarollo.** 2004. Ablation of TrkA function in the immune system causes B cell abnormalities. Development **131:**5185–5195.
7. **Coppola, V., A. Veronesi, S. Indraccolo, F. Calderazzo, M. Mion, S. Minuzzo, G. Esposito, D. Mauro, B. Silvestri, P. Gallo, P. Falagiani, A. Amadori, and L. Chieco-Bianchi.** 1998. Lymphoproliferative disease in human peripheral blood mononuclear cell-injected SCID mice. IV. Differential activation of human Th1 and Th2 lymphocytes and influence of the atopic status on lymphoma development. J. Immunol. **160:**2514–2522.
8. **Dixon, B., B. Sahely, L. Liu, and B. Pohajdak.** 1993. Cloning a cDNA from human NK/T cells which codes for an unusual leucine zipper containing protein. Biochim. Biophys. Acta **1216:**321–324.
9. **Geiger, C., W. Nagel, T. Boehm, Y. van Kooyk, C. G. Figdor, E. Kremmer, N. Hogg, L. Zeitlmann, H. Dierks, K. S. Weber, and W. Kolanus.** 2000. Cytohesin-1 regulates beta-2 integrin-mediated adhesion through both ARF-GEF function and interaction with LFA-1. EMBO J. **19:**2525–2536.
10. **Hofer, S., K. Pfeil, H. Niederegger, S. Ebner, V. A. Nguyen, E. Kremmer, M. Auffinger, S. Neyer, C. Furhapter, and C. Heufler.** 2006. Dendritic cells regulate T-cell de-attachment through the integrin-interacting protein CYTIP. Blood **107:**1003–1009.
11. **Katagiri, K., N. Ohnishi, K. Kabashima, T. Iyoda, N. Takeda, Y. Shinkai, K. Inaba, and T. Kinashi.** 2004. Crucial functions of the Rap1 effector molecule RAPL in lymphocyte and dendritic cell trafficking. Nat. Immunol. **5:**1045–1051.
12. **Kitano, J., K. Kimura, Y. Yamazaki, T. Soda, R. Shigemoto, Y. Nakajima, and S. Nakanishi.** 2002. Tamalin, a PDZ domain-containing protein, links a protein complex formation of group 1 metabotropic glutamate receptors and the guanine nucleotide exchange factor cytohesins. J. Neurosci. **22:**1280–1289.
13. **Laudanna, C., J. Y. Kim, G. Constantin, and E. Butcher.** 2002. Rapid leukocyte integrin activation by chemokines. Immunol. Rev. **186:**37–46.
14. **Mansour, M., S. Y. Lee, and B. Pohajdak.** 2002. The N-terminal coiled coil domain of the cytohesin/ARNO family of guanine nucleotide exchange factors interacts with the scaffolding protein CASP. J. Biol. Chem. **277:**32302–32309.
15. **Meyers, E. N., M. Lewandoski, and G. R. Martin.** 1998. An Fgf8 mutant allelic series generated by Cre- and Flp-mediated recombination. Nat. Genet. **18:**136–141.

16. **Milan, G., A. Zambon, M. Cavinato, P. Zanovello, A. Rosato, and D. Collavo.** 1999. Dissecting the immune response to Moloney murine sarcoma/leukemia virus-induced tumors by means of a DNA vaccination approach. J. Virol. **73:**2280–2287.
17. **Nevrivy, D. J., V. J. Peterson, D. Avram, J. E. Ishmael, S. G. Hansen, P. Dowell, D. E. Hruby, M. I. Dawson, and M. Leid.** 2000. Interaction of GRASP, a protein encoded by a novel retinoic acid-induced gene, with members of the cytohesin family of guanine nucleotide exchange factors. J. Biol. Chem. **275:**16827–16836.
18. **Nourshargh, S., and F. M. Marelli-Berg.** 2005. Transmigration through venular walls: a key regulator of leukocyte phenotype and function. Trends Immunol. **26:**157–165.
19. **Palacios, F., L. Price, J. Schweitzer, J. G. Collard, and C. D'Souza-Schorey.** 2001. An essential role for ARF6-regulated membrane traffic in adherens junction turnover and epithelial cell migration. EMBO J. **20:**4973–4986.
20. **Randazzo, P. A., and D. S. Hirsch.** 2004. Arf GAPs: multifunctional proteins that regulate membrane traffic and actin remodelling. Cell Signal. **16:**401–413.
21. **Rongo, C.** 2001. Disparate cell types use a shared complex of PDZ proteins for polarized protein localization. Cytokine Growth Factor Rev. **12:**349–359.
22. **Rosato, A., V. Bronte, S. Mandruzzato, A. Zambon, F. Calderazzo, G. Biasi, P. Zanovello, and D. Collavo.** 1992. Role of adhesion molecules in the immune reaction to M-MSV-induced tumors. Int. J. Cancer Suppl. **7:**24–27.
23. **Rosato, A., S. Mandruzzato, V. Bronte, A. Zambon, B. Macino, F. Calderazzo, P. Zanovello, and D. Collavo.** 1995. Role of anti-LFA-1 and anti-ICAM-1 combined MAb treatment in the rejection of tumors induced by Moloney murine sarcoma virus (M-MSV). Int. J. Cancer **61:**355–362.
24. **Santy, L. C., and J. E. Casanova.** 2001. Activation of ARF6 by ARNO stimulates epithelial cell migration through downstream activation of both Rac1 and phospholipase D. J. Cell Biol. **154:**599–610.
25. **Smith, A., Y. R. Carrasco, P. Stanley, N. Kieffer, F. D. Batista, and N. Hogg.** 2005. A talin-dependent LFA-1 focal zone is formed by rapidly migrating T lymphocytes. J. Cell Biol. **170:**141–151.
26. **Springer, T. A.** 1995. Traffic signals on endothelium for lymphocyte recirculation and leukocyte emigration. Annu. Rev. Physiol. **57:**827–872.
27. **Tang, P., T. P. Cheng, D. Agnello, C. Y. Wu, B. D. Hissong, W. T. Watford, H. J. Ahn, J. Galon, J. Moss, M. Vaughan, J. J. O'Shea, and M. Gadina.** 2002. Cybr, a cytokine-inducible protein that binds cytohesin-1 and regulates its activity. Proc. Natl. Acad. Sci. USA **99:**2625–2629.
28. **Tessarollo, L.** 2001. Manipulating mouse embryonic stem cells. Methods Mol. Biol. **158:**47–63.
29. **Watanabe, M., K. L. McCormick, K. Volker, J. R. Ortaldo, J. M. Wigginton, M. J. Brunda, R. H. Wiltrout, and W. E. Fogler.** 1997. Regulation of local host-mediated anti-tumor mechanisms by cytokines: direct and indirect effects on leukocyte recruitment and angiogenesis. Am. J. Pathol. **150:**1869–1880.
30. **Weber, K. S., C. Weber, G. Ostermann, H. Dierks, W. Nagel, and W. Kolanus.** 2001. Cytohesin-1 is a dynamic regulator of distinct LFA-1 functions in leukocyte arrest and transmigration triggered by chemokines. Curr. Biol. **11:**1969–1974.
31. **Zanovello, P., E. Vallerani, G. Biasi, S. Landolfo, and D. Collavo.** 1988. Monoclonal antibody against IFN-gamma inhibits Moloney murine sarcoma virus-specific cytotoxic T lymphocyte differentiation. J. Immunol. **140:**1341–1344.